

THE NEW CLOSED CIRCUIT WIND TUNNEL OF THE AIRCRAFT LABORATORY OF UNIVERSITY OF SÃO PAULO, BRAZIL

Catalano, Fernando Martini, PhD
Aerodynamic Laboratory, University of Sao Paulo, São Carlos, Brazil

Keywords: *Wind Tunnel design. low noise fan. low cost aerodynamic facility*

Abstract

This work presents the design and operational range of the new closed circuit Wind Tunnel of The Aircraft Laboratory of The Sao Carlos Engineering School, University of Sao Paulo - Brazil. The working section cross section is 1.29m high and 1.67m wide with a usable length of 3m. The axial fan has eight blades and is driven by a 150Hp AC electric motor controlled by a frequency inverter via a PC computer. The contraction ratio is 1:8 and has two mesh screens at the settling chamber as flow controllers. The two first diffusers are of low diffusion ratio in order to ensure flow free from separation. The necessary diffusion ratio to join with the contraction section is made by a wide-angle diffuser with a curved mesh screen positioned at 30% of its length in order to avoid flow separation. The controlled velocity range is 10m/s minimum to 55m/s maximum and the turbulence intensity is 0.25% suitable for basic aerodynamics and applied aerodynamics tests. Instrumentation is composed of a six component over head balance, scanivalves and digital pressure scans and three-channel hot wire anemometer plus 3-D traverse gear. The working section is equipped with wall boundary layer control for testing high lift 2-D wings.

1. Introduction

In 1994 The Aircraft Laboratory (LAE) started to design a Wind Tunnel as a multi-role experimental facility to attend the needs of the automobile industry based in Brazil. This was proposed as a joint adventure with all carmakers due to their real demand of wind tunnel testing.

It was observed that the main wind tunnel tests usually performed by the automobile industry are divided into 20% pure aerodynamics tests and 80% climatic tests. Therefore, the proposed wind tunnel was of the closed circuit type and with full-scale climatic testing capabilities such as high and low temperature control, sunlight incidence control and anechoic test chamber. The design program included the construction of a 3/8 scale proof of concept wind tunnel model, the construction of which started at the end of 1997. With the globalisation tendency, the carmakers based in Brazil simply stopped all designs or even a proposal of a domestic car model. This indicated that there was no more need, at least temporarily, for wind tunnel tests for the car industry in Brazil. In view of this scenario and with the welcome renewal of EMBRAER the Aircraft Laboratory decided to modify the original design of the 3/8 scale model in order to construct a pure aeronautical wind tunnel, while maintaining the possibility of testing racing car models.

When designing a new wind tunnel, a parametric study must be carrying out in order to avoid a bad design, which could result in a wind tunnel with a chronic flow problem. In order to perform this study a special program of visits was made in 1996 when a group of researchers of LAE visited major wind tunnel facilities around the world. One of the most advanced facilities visited was the DNW wind tunnel. This fantastic wind tunnel is without doubt the best low speed wind tunnel in the world. It has four types of changeable working sections, a huge moving ground and a variety of aerodynamic balances which are suitable for most of the experimental work in aeronautics,

ground vehicles and civil constructions. The aerodynamic circuit was carefully designed to efficiently extract the 12.5MW from the motor. Such a wind tunnel was the basis for the LAE wind tunnel design. The size of the LAE wind tunnel was calculated in order to keep the Reynolds Number as high as possible for low speed applied aerodynamics testing with the lowest power needed. This work describes the LAE wind Tunnel design process and construction details.

2. Design Philosophy

As pointed out above, the LAE wind tunnel design was based on the DNW wind tunnel layout. This includes low diffusing angles at the main diffusers and a wide-angle diffuser placed just before contraction cone. This would ensure separation free diffusion for the main diffusers. Separation at the diffuser is the main source of working section velocity oscillations and are usually of difficult solution. In the other hand, wide-angle diffusers can be efficiently designed to avoid separation by using mesh screens. This layout is also convenient because it is possible to design corner ducts with the same dimensions, so that, corners 1 and 2 are exactly the same as are corners 3 and 4. Corner sections with the same size means also ease of construction and, more important, the same corner vanes. Corner vanes are difficult to make and need careful assembly to avoid separation by using mesh screens. This layout is also convenient because it is possible to design corner ducts with the same dimensions, so that, corners 1 and 2 are exactly the same as are corners 3 and 4. Corner sections with the same size means also ease of construction and, more important, the same corner vanes. Corner vanes are difficult to make and need careful assembly to avoid flow distortions and large pressure losses. The corner vanes were one of the more carefully designed items of the circuit due to the cost in money and in pressure drop. It was decided to use the classical Collar's [1] profile for the corner vanes that, despite of the complex shape give the lowest pressure drop. The

contraction ratio was kept to 1:8 due to building space limitation. Although it was considered large enough to damp turbulence and promote low speed at the contraction entrance-settling chamber where the mesh screens are installed. The complete circuit has corner fillets to prevent secondary vortices at the wall junctions, but the cross section geometric shape is not considered octagonal. The fan section has a static front spinner and a long rear body, which accommodates the electric motor and transmission system. The fan has eight blades with a hub to fan ratio of 1:2.2, and seven straighteners to damp flow rotation. The blades were designed for high efficiency and low noise and were made in composite to assure low fan inertia for fast stopping in the case of an emergency. The working section has no corner fillets, one main door and two secondary doors for quick access to the model. It was decided to not put corners fillets at the working section due to two reasons: first for facilitate the construction and substitutions of wall panels when it is necessary (it is always necessary in a wind tunnel life), and second because of the corner fillet interference on half models. It was just a case of cost and benefit: for a certain pressure loss there will be some advantages as pointed out. The working section is involved by a room or plenum chamber, which is used as a pressure equalizer in order to maintain atmospheric pressure inside the working section by means of lateral vents.

3. Circuit Design

It was decided to initiate the design of the main circuit dimensions from two previous specifications: a) the working section dimensions and b) the contraction ratio. As pointed out before, the wind tunnel dimensions were limited by the room space available in the Laboratory so that the working section main dimensions were fixed at 1.29m high, 1.67m wide and 3 m long. For the same reasons the contraction ratio was limited to 1:8 so that the contraction inlet dimensions are 4.72m wide to 3.65m high. The contraction cone length was

calculated by its aerodynamic design and was fixed at 4m in order to avoid boundary layer separation. With these dimensions the corners, the diffusers and the fan section could be designed. Therefore, the contraction, the working section and first diffuser could be placed inside the LAE building without compromising the whole laboratory space, see **Fig. 1**. **Table 1** gives the main dimensions of each circuit section, where A1 and A2 are inlet and exit section areas respectively, L the section length, A2/A1 diffuser or contraction ratio and 2ϕ the diffuser equivalent cone angle.

Table 1 - Main circuit dimensions

Section	A1(m ²)	A2(m ²)	L (m)	A2/A1	2φ (deg)
Working section	2.15	2.35	3.00	1.1	1.40
1 st Diffuser	2.35	3.90	5.78	1.67	4.94
Corners 1 and 2	3.90	3.90	8.85*	0	0
Fan section (2.4m diam)	3.9	3.9	6.54	0	0
2 nd Diffuser	3.9	7.87	11.5	2.02	6.7
Corners 2 and 3	7.87	7.87	9.94*	0	0
Wide angle Diffuser	7.87	17.22	2.7	2.2	30.6
Settling Chamber	17.22	17.22	2.0	0	0
Contraction	17.22	2.15	4.0	8 (CR)	-

* center line length



Figure 1 Wind Tunnel position with reference to the Laboratory room space.

4. Fan Design.

Fan design was based on a modification of the methodology of Bruno Eck [2] with some

suggestions given by Alan Pope [3]. The main modification of these methods was made on the calculation of the blade aerodynamic characteristics. A computer program was used which includes a viscous analysis. The other important modification was of the blade aerodynamic profile. Due to the advanced aerodynamic calculation a type of profile was used that was especially designed to cope with the fan operational Reynolds Number and effective incidence angle without any concern to the blade model construction. In the past, flat bottom surface airfoils such Clark Y or RAF types, were used because of their ease of construction. Today with the advent of rapid prototyping, the complex blade shape can be reproduced in hours in order to perform the construction of the blades using composite modeling. The fan design was based on two constraints: high efficiency and low noise. It obvious in this case that low noise is only achieved with an aerodynamically well-designed fan since the main sources of fan noise is airflow born. An aerodynamic profile of the Eppler family was chosen (the Eppler 662), due to high performance at low Reynolds and the capacity to create high lift to drag at low incidence angles as the blades always operate at low incidences. The fan final geometric and aerodynamic characteristics are plotted in **Fig. 2** where c , L/D and β are the blade local chord, section lift to drag ratio and pitch angle respectively. The pitch (twist) angle of the blade is with reference to the root section. The axis of twist is located at the centre of each section (instead of the usual $\frac{1}{4}$ chord) for symmetry reasons, which facilitate the fan boss construction. The fan diameter is 2.4 metres and the blade span 0.6 m which gives a fan to boss diameter ratio of 0.5. The front spinner is elliptic and does not rotate with the fan. The rear body has an aerodynamic shape to promote a slow annular expansion of the fan downstream flow and to accommodate the electric motor, fan shaft and bearings. The flow straighteners have a NACA profile and a trapezoidal planform with a chord of 0.5m at the spinner and 1.0m at the tunnel wall. A total of seven straighteners were designed as the fan has eight blades, to avoid

sound resonance. **Fig. 3** shows the fan section with the front and rear spinners, motor and drive system as well as the flow straighteners and **Fig. 4** shows the fan ready to run.

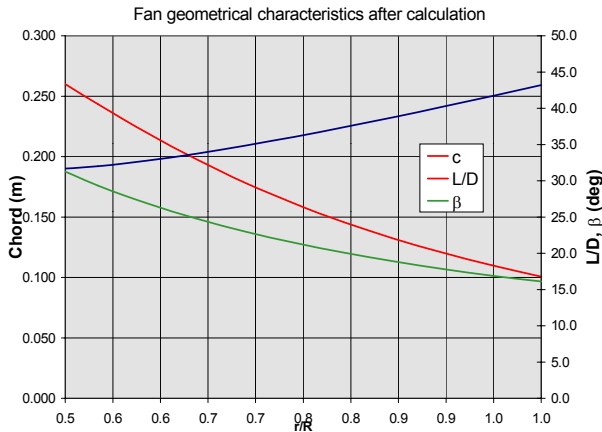


Figure 2 Lift to drag distribution and geometric characteristics of the blade.

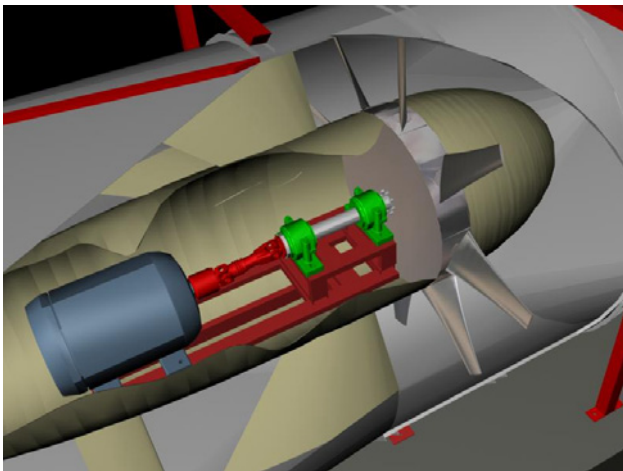


Figure 3 Fan section and motor drive system.



Figure 4 Fan final configuration.

5. Corner Vanes Design

It was decided to be conservative with respect to the corner vanes design to avoid difficulties in construction and unnecessary flow problems. First of all it was necessary to choose vane profile, which would be easy to manufacture and provide good turning flow with low-pressure loss. Such a vane profile is not easy to design because it is virtually impossible to have all these advantages at same time. But it was decided to use an aerodynamic profile of the Collar type [1] for the vanes in order to maintain good flow quality and low pressure loss, despite the fact they are of complex construction. The construction was executed using a fiberglass mold to laminate all the corner vanes also in fiberglass. This procedure made sure that all the vanes are equal in shape, smooth and, above all not expensive to build. To avoid noise resonance and vibration, all the corner vanes were filled with polyurethane foam. **Figure 5** shows a comparison between various corner vane types in respect to the total head loss coefficient, $\delta(t,h)/q_{ic}$ as a function of the gap/chord ratio. As it can be seen in **Figure 5** the best gap/chord ratio is 0.4 for the Collar's vanes. Therefore, 13 corner vanes were used at each corner section, as the vane chord and section length are 0.40/3.25m and 0.54/4.58m for the first and second two corners respectively.

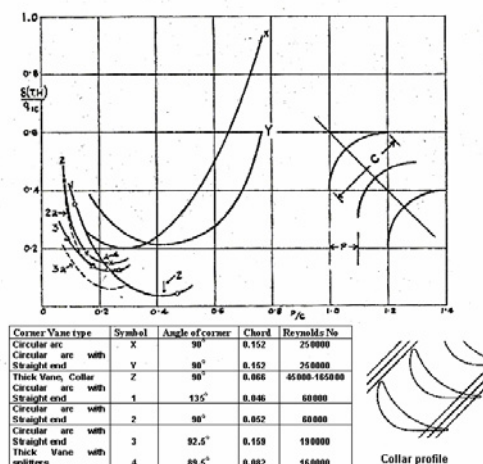


Figure 5 Comparison between various corner vanes in respect to loss and gap between vanes (Salter [4]).

6. Contraction Cone

The contraction cone has a 1:8 contraction ratio and is 4.0 m long. It was designed using Morel 's [5] technique. This technique uses two cubic curves (Equation 1) separated by a inflection point located in some particular position which is determined by flow uniformity and boundary layer safety considerations. In this case it was decided to locate the inflection point at 60% of the distance from the cone entrance. **Fig. 6** shows the lateral view of the contraction cone. The settling chambers at the inlet and exit of the contraction are 1.8m and 0.8m long respectively.

Two mesh screens of 1.7 mm mesh and porosity of 0.54 are located at the inlet settling chamber separated by 0.25m (Catalano [6]). Also, both settling chambers are fitted with static pressure rings for velocity measurements.

$$\frac{D}{D_1} = 1 - F_i \left(\frac{x}{D_1} \right)^3 \quad (1)$$

Where D_1 is the inlet hydraulic diameter, D is the diameter at x position and F_i is a function of the contraction ratio m , the inflexion point X and the length L of the contraction defined by:

$$F_i(\text{inlet}) = \frac{m-1}{m} X^{-2} \left(\frac{L}{D_1} \right)^{-3} \quad \text{and} \quad (2)$$

$$F_e(\text{exit}) = \frac{m-1}{m^3} (1-X)^{-2} \left(\frac{L}{D_1} \right)^{-3}$$

To keep boundary layer safe and as thin as possible, Morel suggests that:

$$0.75 \leq \frac{L}{D_1} \leq 1.25 \quad \text{and} \quad 0.2 \leq X \leq 0.8$$

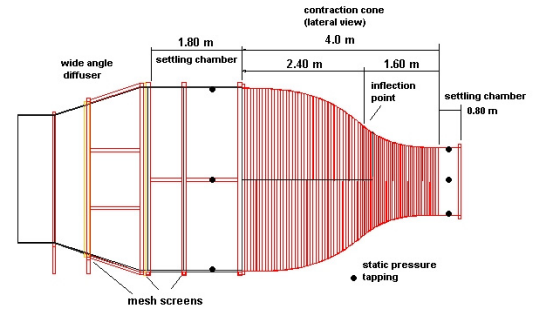


Figure 6 Contraction cone

7. Circuit Energy Loss calculation

The circuit energy losses were calculated for each section separately and referenced to the working section flow conditions. Each local loss parameter is calculated based on local conditions at the smallest area end of each section and then referenced to the test section condition using the **Equation 3** (Eckert et al [7]). K is the pressure loss, A smallest-end area, M is the Mach number at this section and γ is the air specific heat ratio. The subscript 'o' means values at the working section.

$$K_o = \left[\frac{A_o M}{A M_o} \sqrt{\frac{1 + \left(\frac{\gamma-1}{2} M_o^2 \right)}{1 + \left(\frac{\gamma-1}{2} M^2 \right)}} \right]^2 \quad (3)$$

The energy ratio of the wind tunnel is given by:

$$ER = \frac{1}{\sum_{i=1}^n K_{oi}} \quad (4)$$

The power required to be input into the flow in order to drive the flow through the wind tunnel at a specific working section velocity is given by **Equation 5**, where ρ is the air density in Kg/m^3 and V the velocity in m/s.

$$P_{input} = \left(\sum_{i=1}^n K_{oi} \right) \rho_o^2 A_o V_o^3 \quad (5)$$

The power required is dependent on the efficiency of the fan, motor and drive system.

With η_f as the fan system efficiency the power required is:

$$P_{required} = \frac{P_{input}}{\eta_f} \quad (6)$$

Table 3 summarizes each section local pressure loss and with reference to the working section conditions. The working section conditions set for the calculations were: $V_o = 50$ m/s, $\rho_o = 1.2$ Kg/m³ at an average temperature of 299 °K.

Table 2 Pressure loss coefficients for each section referenced to the working section conditions.

Section	A(m ²)	V(m/s)	K _o
Working section	2.15	50	0.015
1 st Diffuser	2.35	27.56	0.009
Corners 1 and 2	3.90	27.56	0.10
Fan section (2.4m diam)	4.5	23.88	.057
2 nd Diffuser	3.9	27.56	0.008
Corners 2 and 3	7.87	13.65	0.07
Wide angle Diffuser	7.87	13.65	0.005
Mesh screens (2)	17.22	6.24	0.024
Settling Chamber	17.22	6.24	0.0002
Contraction	17.22	50	0.0023
		$\sum_{i=1}^n K_{oi}$	0.2905
		P_{input} (W)	58100
$\eta_f=80\%$		$P_{required}$ (W)	72625

From **Table 2** it can be seen that some energy reserve still remains in order to overcome further energy losses due to model blockage and the uncertainties of the circuit friction drag calculations. A smooth walled wind tunnel was considered but in reality there are protuberances, small gaps and geometric asymmetry.

The tunnel circuit has the wall panels carefully jointed and the screw holes filled in order to avoid protuberances and gaps. Also there are corners filets to avoid the formation secondary flow between the walls in all circuit length except at the working section.

8. Construction

Because of the relatively low budget for construction of the wind tunnel, it was decided to carry out a low cost construction but at the same time robust enough to keep the tunnel working for the next 20 years with an annual maintenance program. A 2cm thick water resistant plywood coated on both faces with resin was chosen for the wall panels at all section except for the contraction cone, in which naval plywood of 5mm thickness was used. The 2cm thick plywood is 1.1m wide by 2.2m long and the wall panel size were kept close enough to these dimensions to avoid loss and excess cutting. The external structure was made of a 6cmx6cm squared section metal tube welded to form rings. The plywood wall panels were fixed to the metal structure using bolts, washers and nuts. More of 6.000 bolts were used on the circuit construction.

The working section has a front wall fitted entirely as a door in order to provide enough room to put models inside the test section. This big door is made of a metal structure with an acrylic wall to provide wide vision from outside. There is also a small door in both vertical walls for model checks without the need to move the big door. The length of the working section was calculated using Pope's [3] suggestion, which should be one to two times the major dimension of the jet. The working section also has a small diffusion of about 1 degree at the ceiling and vertical walls (Pankhurst et al [8]). The floor was kept as horizontal as possible to be used as reference to set the models. **Fig. 7** shows the working section from outside and inside (downstream).



Figure 7 Working section.

The complete working section is located inside a room, which acts as a plenum chamber

to equalize pressure. This plenum is made of concrete and has a control room from which the tunnel and all the testing will be controlled avoiding noise and discomfort. As pointed out before, the corner vanes were made of fiber glass filled with polyurethane foam and a wood rib at each end in which were fixed two screws: one at $\frac{1}{4}$ chord for adjustments and the other to fix the vane in position. Fig. 8 shows the first corner vane section.



Figure 8 First corner vane section.

The mesh screen is of the nylon type, which has been tested and used for a long time at LAE (Catalano [9]). The fan has two circular metal plates to which the blades are fixed. The blade-fixing element is made of solid wood and the blades pitch angle may be adjusted if necessary before running. Fig. 9 shows the assembling of the fan blades.



Figure 9 Blade/boss assembling.

9. Flow Characteristics and Calibration.

A series of hot wire mapping were carried out in order to determine the working section flow characteristics. The turbulence intensity was first measured from a fixed single gold plated hot wire probe. The results are shown in Fig. 10.

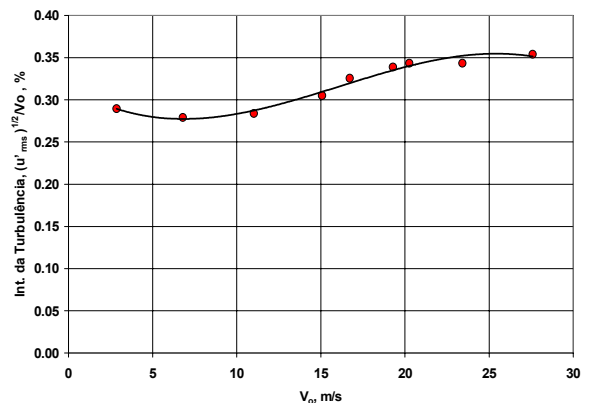


Figure 10 Turbulence intensity.

Also, a turbulence spectrum was calculated showing that there was no high pick of the turbulence spectrum for any range of frequencies. Fig. 11 shows the turbulence spectrum for 22.5m/s.

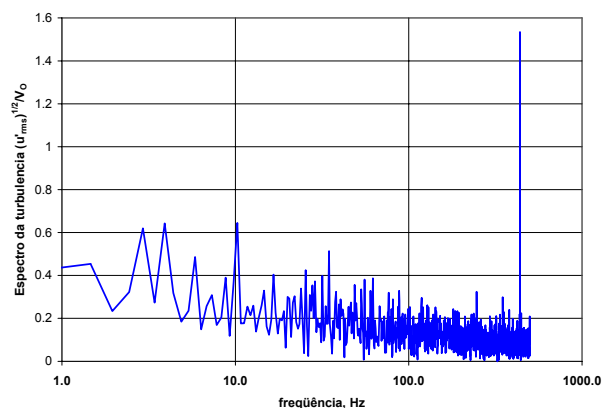


Figure 11 Turbulence spectrum for $V_0=22.5\text{m/s}$.

Velocity non-uniformity was calculated based on vertical and horizontal mapping at center of the working section. The results for low velocity where keeping uniform velocity distribution at working section is more difficult are presented at Table 3. Where ϵ_x and ϵ_q are

the longitudinal velocity and dynamic pressure non-uniformities respectively.

Table 3 Longitudinal velocity and dynamic pressure non-uniformities.

Velocity V_0 , m/s	Frequency, Hz	ϵ_x , %	ϵ_q , %
11,1	0,5 – 30K	0,50	0,39
18,5	0,5 – 30K	0,89	0,77

Power consumption versus working section velocity was measured as well as the wind tunnel power factor. These results are presented in Figs. 12 and 13 respectively.

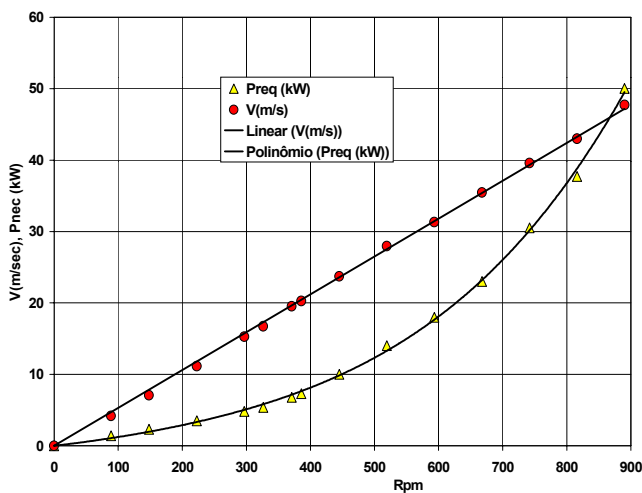


Figure 12 Power consumption and velocity versus fan rpm.

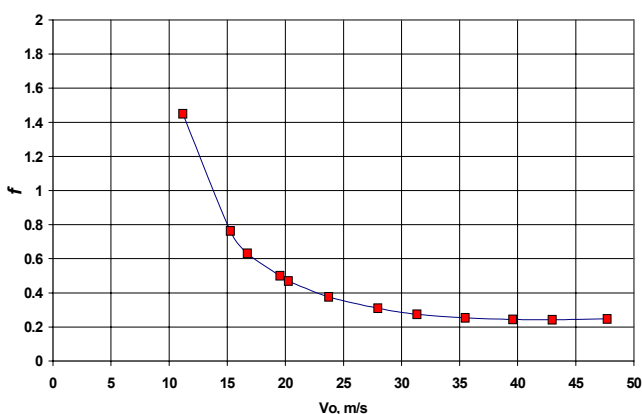


Figure 13 Wind tunnel power factor.

10. Conclusions

The design and construction and calibration details of the new LAE closed circuit wind tunnel are presented. Cost effective design and construction is possible when local materials are adopted and innovative fabrication processes are used. It really is not necessary to spend great amounts of money to construct a medium size wind tunnel, which provides a valuable test facility. Money may be saved in construction, even when robustness is required, by using a combination of materials. By saving money in this way it is possible to invest more in instrumentation, such as fast data acquisition and a good aerodynamic balance. The fan design is crucial for keeping down the motor and controller costs since less energy is necessary in operation of a well-designed fan.

References

- [1] Collar A.R. "Some Experiments with Cascade of Airfoils", *R&M* 1768 1937.
- [2] Eck, B. "FANS Design and Operation of Centrifugal, Axial-Flow and Cross Flow Fans" Pergamon Press 1973.
- [3] Pope A. & Harper J. J. "Low Speed Wind Tunnel Testing" John Wiley & Sons, Inc New York 1966.
- [4] Salter C. "Experiments on Thin Turning Vanes *Reports and Memoranda* No. 2469 25th October 1946
- [5] Catalano, F.M "Design, Construction and Calibration of a Open Circuit Wind Tunnel of N.P.L. Type and Hexagonal Cross Section, MsC Theses, EESC/University of São Paulo 1988.
- [6] Morel, T. "Comprehensive Design of Wind Tunnel Contractions", *Journal of Fluid Engineering*, ASME Transactions, pp. 225-233, June 1975.
- [7] Eckert W.T.,Mort K.W & Jope J., "Aerodynamic Design Guidelines and Computer Program for Estimation of Subsonic Wind Tunnel Performance" *NASA Technical Note TN D-8243* October 1976.
- [8] Pankhurst, R. C. & Holder, D. W. "Wind Tunnel Technique", Sir Isaac Pitman & sons LTD London, 1968
- [9] Catalano, F.M. "Características Aerodinâmicas de Telas Comerciais de Nylon" ABCM X COBEM Dezembro 1989
- [10] Gorlin, S. M. & Slezinger, I. I. "Wind Tunnel and Their Instrumentation" Israel Program for Scientific Translations LTD , NASA TTF-346 TT 66-51026, 1966.